Universiti Malaysia Terengganu Journal of Undergraduate Research *eISSN: 2637-1138*
Volume 4 Number 2, April 2022: 37-50

PARAMETRIC STUDY ON WAVE OVERTOPPING DUE TO WEDGE ANGLE AND FREEBOARD OF WAVECAT WAVE ENERGY CONVERTER

MOHAMAD IZZUL, MOHAMMAD FADHLI*, MOHD AZLAN AND MOHD NOOR

Faculty of Ocean Engineering Technology and Informatics, Universiti Malaysia Terengganu, 21030 Kuala Nerus, Terengganu, Malaysia

**Corresponding author: fadhli@umt.edu.my* *https://doi.org/10.46754/umtjur.v4i2.273*

Abstract: Wave energy presents great potential in many coastal regions. This paper deals with WaveCat, a new wave energy converter (WEC) recently patented by the University of Santiago de Compostela. The WaveCat has two hulls, like a catamaran, and it operates according to the overtopping principle. The higher the overtopping amount collected in the reservoir, the higher the energy generated. The wedge angle and freeboard are two important parameters that contribute to a higher overtopping discharge. However, knowledge on the influence that wedge angle and freeboard have on wave overtopping is limited. Hence, this study aims to extend the borders of available knowledge by investigating the influence that two parameters have on wave overtopping discharge through simulation using computational fluid dynamics (CFD). The WEC was designed in the AutoCAD software. Then, the parameters were simulated using CFD. The parameters of wave height and wave period with a specified range are added and the relationship between wedge angle, freeboard and wave overtopping performance of WaveCat were analysed. The validation results showed good agreement between the simulation and physical experiment, with a percentage error of within 20%. The results are useful for further investigation related to optimising WaveCat parameters for selecting the best performance.

Keywords: Wave Overtopping, Wave Energy Converter, Wedge Angle, CFD

Introduction

The heavy consumption of fossil fuels has well-known environmental impacts, so the contribution of renewables to total energy output needs to be increased as quickly as possible. In this context, several regions and countries around the world have set new goals for renewable energy, for example 20% of renewable energy in the European Union by 2020, or 30% in Denmark by 2050 (Mathiesen *et al.,* 2015). To achieve these goals, the contribution of the renewable energies currently being used, such as wind or photovoltaics, must be increased and the new renewable energies that are not yet being commercially utilised (or barely so) should be produced. Wave energy is among the most promising of the latter (IRENA, 2014).

The winds blowing over the ocean surface create ocean waves, so wave energy can be perceived as a concentrated form of wind energy (Sun *et al.,* 2018). Wave energy has a number of advantages compared with other renewables: high resource predictability, high power density, relatively high consumption factor, and low environmental and visual effects. For these reasons, wave energy is widely considered as one of the renewable energy sources with the greatest development potential. According to the European Science Foundation, Europe may meet up to 50% of its electricity demands from marine renewable energy by 2050 (Rusu *et al.,* 2008). Intensive research is dedicated to wave energy resource assessment in many regions around the world (Astariz & Iglesias, 2015; Contestabile *et al.,* 2015; Cornett, 2009; Folley & Whittaker, 2009; Haas *et al.,* 2011; G. Iglesias & Carballo, 2010; Jarocki, 2010; Shih *et al.,* 2018; Waters *et al.,* 2009).

WaveCat is an offshore floating wave energy converter (WEC) with oblique wave overtopping as its operating concept as shown

in Figure 1. It consists of two hulls (hence its name), like a catamaran. Unlike a catamaran, however, the hulls do not converge in parallel, but form a wedge in the view of the plane; they are connected at the stern by a character that causes the angle between them to differ depending on the state of the sea. The freeboard and draught can also differ depending on the state of the sea.

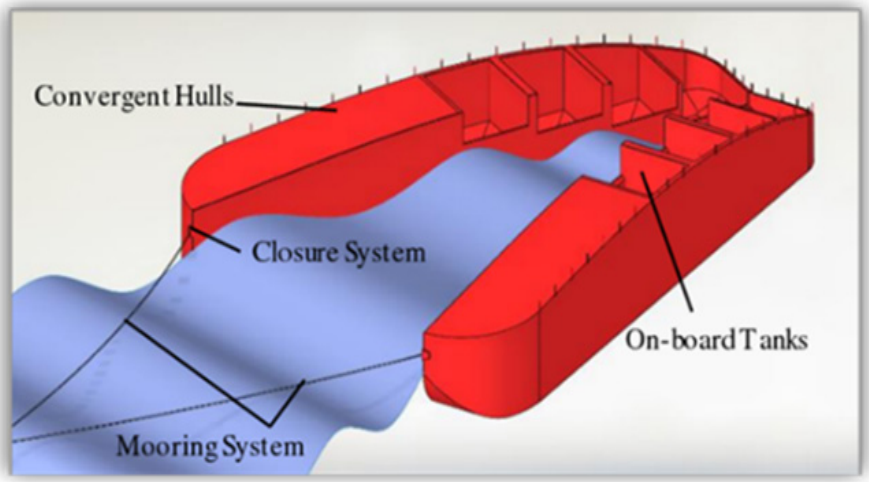

Figure 1: A schematic of the WaveCat concept (Iglesias *et al.,* n.d.)

In addition, the freeboard varies with the length of each hull, decreasing towards the stern so that overtopping continues as the wave propagates between the hulls (with a constant freeboard, decreasing the height of the wave crest due to the initial overtopping may disrupt overtopping before the wave reaches. The prototype's total length is 90 m. WaveCat is intended to operate offshore at water depths ranging from 50 m to 100 m, where the wave energy supply is greater than nearshore or onshore. Another benefit of offshore deployment is the low environmental impact of nearshore or onshore WECs, and in particular WaveCat's low visual impact due to its floating existence and lack of superstructures.

Materials and Methods

The study starts with the validation of the wedge angle to the overtopping discharge through simulation. In order to achieve this, tests were carried out using different wedge angles. Constant wave conditions were used in the tests. After the simulation is completed, the results of the tests were analysed and compared with the experimental results.

CFD Modelling

Computational fluid dynamics (CFD) is a method of simulating the process of a flow in which standard flow equations, such as the Navier-Stokes and continuity equations, are discretised and solved for each computational cell. Using a CFD software is in many ways similar to setting up an experiment. If the experiment is not set up correctly to simulate a real-life situation, then the results will not reflect the real-life situation (Baquerizo *et al.,* 1998).

There are numerous branches of physical science that rely on the applications of CFD, including heat transfer, radiation, nuclear reaction, electromagnetic field, oceanography and vascular medicine. Based on the field of fluid mechanics, general CFD studies include

nonlinear waves, viscous effects, green water effects, slamming loads and wave breaking (Cornett, 2009). In recent years, researchers have studied wave hydraulics behaviours and structural design performance, mostly in the aspect of wave overtopping discharges by using various types of CFD software, which can be seen in studies by Contestabile *et al.* (2015), G. Iglesias and Carballo (2010), and Jarocki and Wilson, (2010).

Methodology of the Study

In every CFD case, validation is used to assess how accurately the computational results compare with the experimental data. For that reason, in geometrical construction using computed-aided design (CAD) programmes, all these geometries have been reconstructed using structural design parameters, the same as previous experiments. The workflow diagram that provides a summary of the CFD studies is shown in Figure 2. The first phase is designing the model of the WaveCat with different wedge angles that will be used in the simulation. The WaveCat with different wedge angles are designed using AutoCAD 2018. For this research, the model was constructed at a scale of 1:30 to test in numerical simulation. The dimensions of the model are shown in Table 1.

Table 1: The orinciple dimensions of WaveCat

Measurement	Details
Length (mm)	3000
Width (mm)	400
Height (mm)	400
Freeboard (mm)	40
Draught (mm)	180

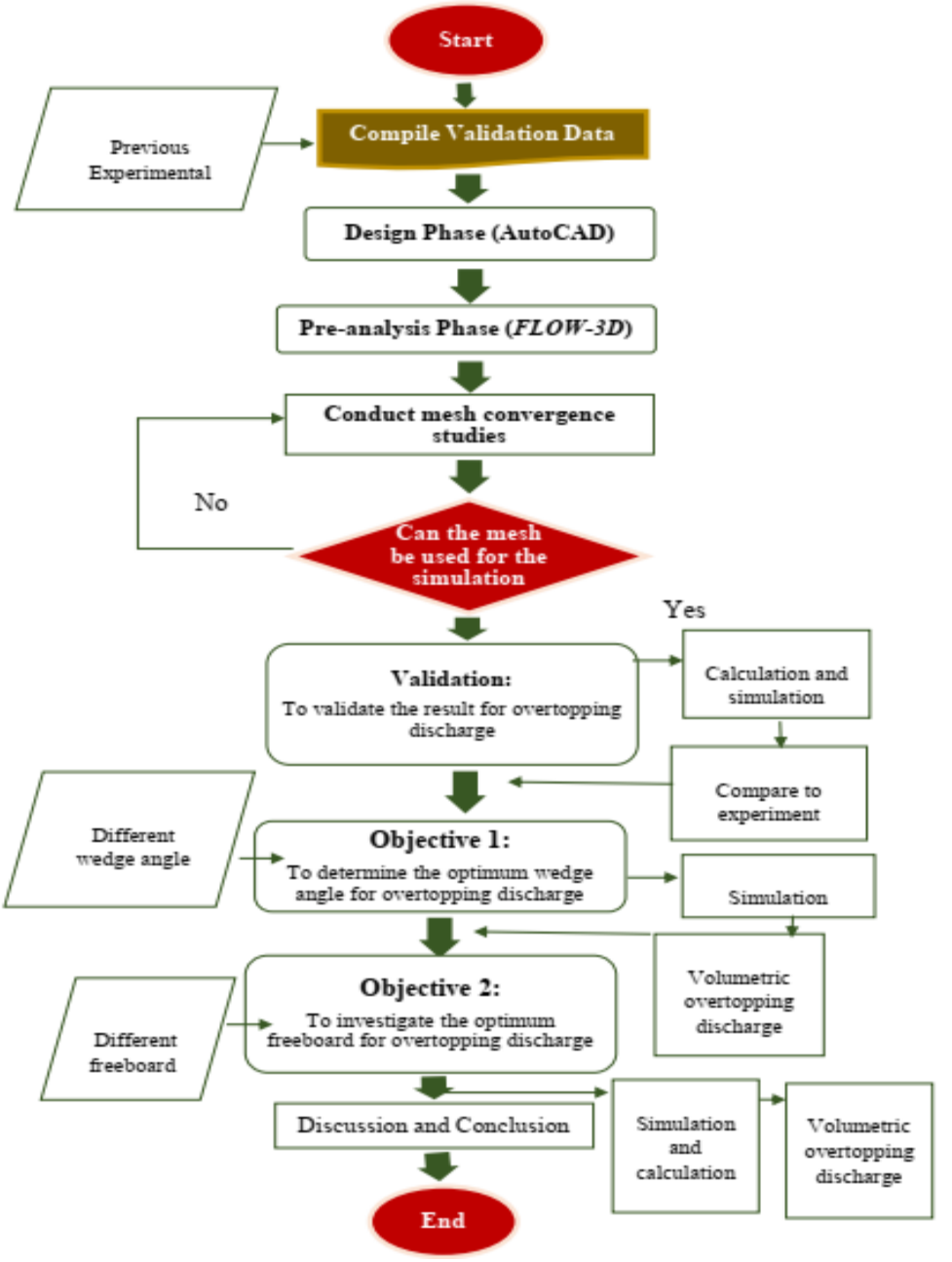

Figure 2: Workflow diagram of the studies

In this study, the WaveCat has been designed exactly the same as in the sketch from the previous study (Iglesias *et al.,* n.d.). The sketch of the dimensions used in this model is presented in Figure 3, and the designed model is shown in Figure 4.

A numerical wave flume was set up to carry out the numerical simulation based on typical experimental arrangements, which consists of a length of 17.46 m for the x-direction, 4 ms in the y-direction and 0.9 m in the z-direction. The general mesh block domain represents the area where the fluid flows, while the local mesh block domain represents the area of structural geometry to be located. The ratio between fine to coarse mesh is 1:2 as suggested by FLOW-3D. For this study, the mesh size for the general mesh (coarse domain) was chosen to be 0.04 the size of cell, 17.46 m × 4 m × 0.9 m, while the local mesh (fine domain) is 0.02 the size of the cell at 3.3 m × 3.6 m × 0.1 m.

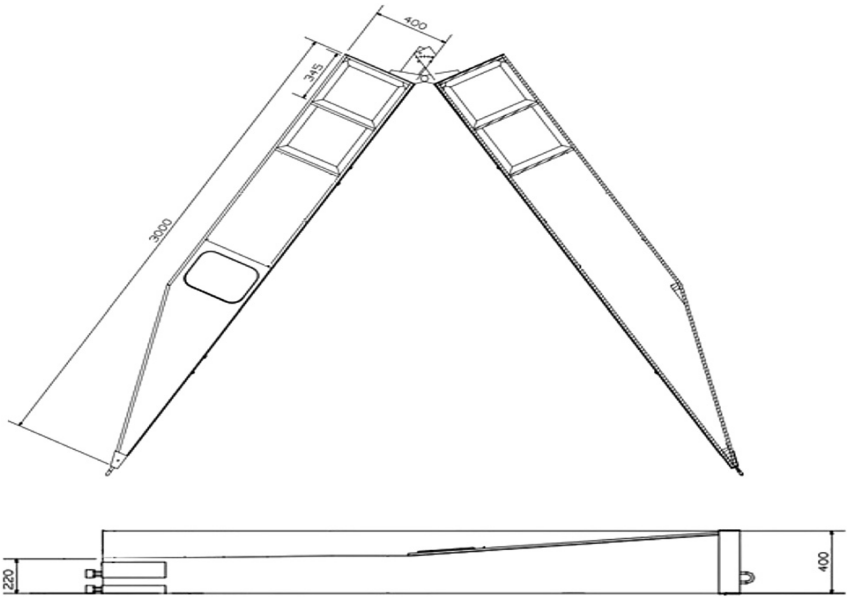

Figure 3: The plan and lateral views of the model (dimensions in mm and model scale)

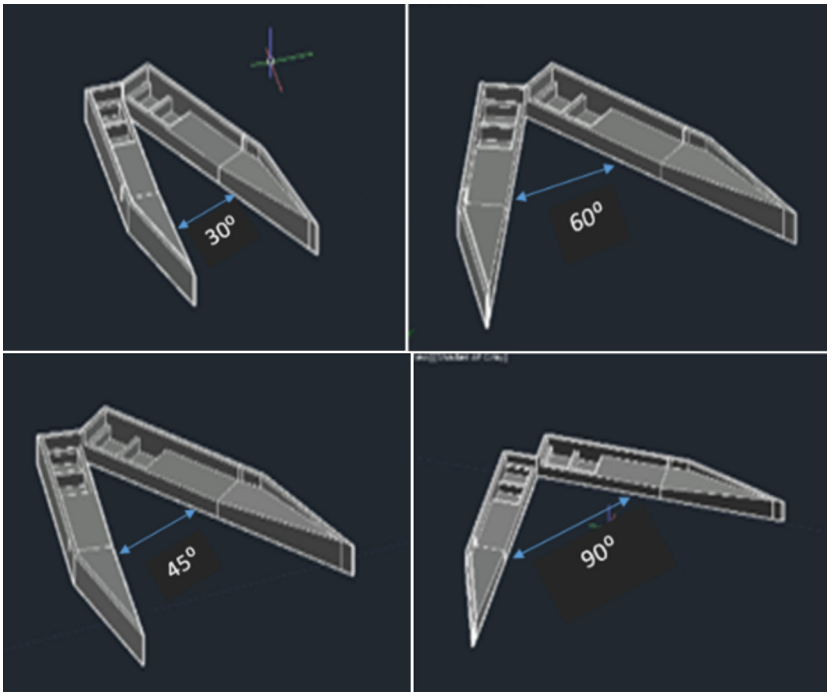

Figure 4: The WaveCat model design for each angle

The Governing Equations for Data Analysis

The greatest influences on the design of a WEC are the hydraulic overtopping procedure. The overtopping manual provides management guidelines on the analysis and estimation of the overtopping discharge volume. Besides that, there has been little research on the role of the overtopping parameter in the design of a WEC. A few overtopping studies have been conducted involving seawalls (Deilami-Tarifi *et al.,* 2016), and one study involved a WEC called Wave Dragon in a laboratory test of ramp angles, profiles and crest freeboard levels (Tedd, 2007). When comparing the results between different scales of models, it is very useful to use non-dimensional units to describe the variables. The results from the model scale can be used for any size of the device. The non-dimensional formula used by Van der Meer (2002) is shown in Equation 1.

$$Q^* = \frac{q}{\sqrt{g}H_s^3} \quad [1]$$

Where :

Q* is the non-dimensional overtopping discharge

q is the dimensional overtopping discharge *($m^2/m/s$)*

g is gravitational acceleration *(m/s^2)*

H_s is the significant wave height *(m)*

The non-dimensional overtopping rate is compared to the relative crest freeboard R to evaluate the overtopping flow efficiency, as shown in Equation 2.

$$R^* = \frac{R_c}{H_s} \quad [2]$$

Froude Models

Froude models denote supplying Froude numbers to the model and the prototype. Open channel models are constructed as Froude models since the motive force in open channels is the gravity force, which is the weight of water in the flow direction. Dam, spillways, harbours,

water intake structures and energy dissipators are examples of hydraulic structures (Tumin *et al.,* 2010). The discharge scale can be found as Equation 3:

$$Q_r = L_r^{5/2} \quad [3]$$

Where:

L_r is the length scale of the model

Q_r is the overtopping discharge of the model

Comparison between the Experimental Results

The data that have been collected in Objective 1 was used to calculated the average overtopping discharge. Then, this data were scaled up by using the Froude model formula. This simulation results were analysed and compared with the experimental data. The standard percent error formula was used to determine the precision of the results calculated. The percentage error formula is shown in Equation 4.

$$\%_{error} = \left(\frac{experimental - theoretical}{theoretical}\right) \times 100 \quad [4]$$

Results and Discussion

The results obtained from the simulation on the effects of different wedge angles on the overtopping discharge are discussed further in this section. Firstly, the results from the simulation were validated with the physical experiment data. Next, the optimum wedge angle that leads to the highest overtopping discharge was chosen. Lastly, the optimum wedge angle was tested with different freeboards to get the highest overtopping discharge between them.

Validation of the Wedge Angle to the Overtopping Discharge

The simulation results were validated with the physical experiment data from Fernandez *et al.* (2012). The percentage error was calculated using Equation 4 for non-dimensional overtopping discharge against the wedge angle. As listed in Table 2, the percentage error decreased as the wedge angle increased, in which the minimum error is close to -8.48%. The value for both simulated and experimental results also decreased and did not differ too much.

Table 2: Overtopping discharge for each wedge angle

Wedge angle (°)	Numerical data (m^3/s)	Experimental data (m^3/s) (Fernandez *et al.*, 2012)	Percentage error %
30	2.28	1.98	-15.28
45	3.21	2.84	-12.95
60	3.57	3.24	-10.24
90	1.16	0.99	-8.48

The graph in Figure 5 shows the same pattern for both simulation and experimental results. The graph shows thta the amount of average overtopping discharge in the reservoir increased from angles 30° to 60°, but decreased at angle 90°. Hence, the results showed good agreement between simulated results and experimental results.

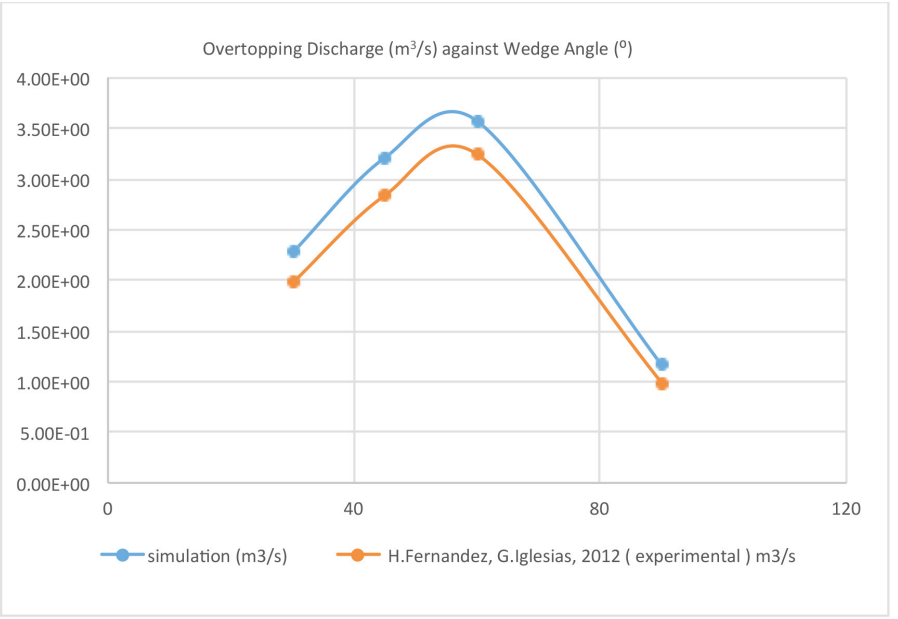

Figure 5: Comparison between physical experiment and numerical simulation results for overtopping discharge versus wedge angle

The main difference between the simulated and experimental results is due to the difficulties in defining the real situation during numerical simulation configurations. It is assumed that the experimental results represent the real behaviour of the object or model, while the simulation results represent the same object based on its theoretical probability. Based on the graph in Figure 5, the simulated results had a percentage error that is lower than 20%. Hence the simulated results had a close relation with the experimental results.

Optimum Wedge Angle for Overtopping Discharge

The total overtopping discharge is obtained through simulation by using four different wedge angles. The freeboard, wave height and wave period were fixed. The overtopping discharge is strongly affected by the wedge angle. Table 3 shows the wedge angle used in the simulation tests.

Table 3: Wedge angle input

Test ID	Wedge angle (°)
A	30
B	45
C	60
D	90

Table 4 shows the results for the dimensional and non-dimensional overtopping discharge for different wedge angles.

Table 4: Overtopping discharge for each wedge angle

Test ID	Wedge Angle (°)	Significant Wave Height, *(m)*	Period T_p *(s)*	Overtopping Discharge	
				q (m³/s)	*Q**
A	30	0.1	2.2	2.28	23.02
B	45	0.1	2.2	3.21	32.41
C	60	0.1	2.2	3.57	36.04
D	90	0.1	2.2	1.16	11.71

Figure 6 illustrates the non-dimensional wave overtopping rate in the reservoir of the simulated results. The distribution of the simulated data plotted in the graph is calculated using Equation 1.

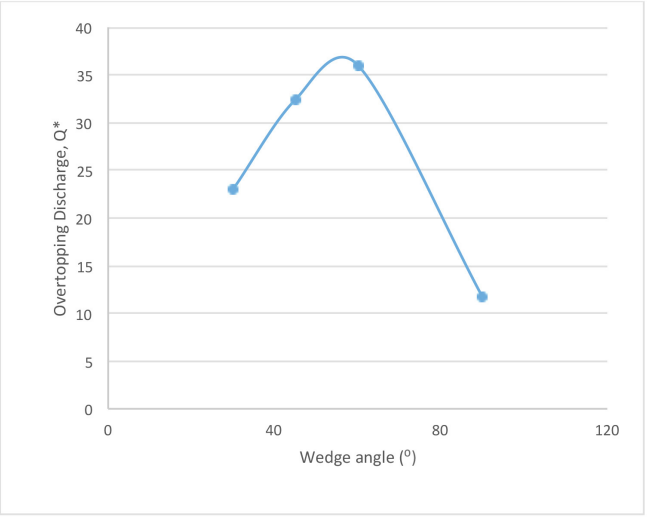

Figure 6: Non-dimensional average overtopping discharge against wedge angle

According to the graph in Figure 6, the best results were obtained with the intermediate values of the angle between hulls of 45° and 60°. In this simulation, the wave conditions used is (= 0.1 m, = 2.2 s) and the optimum value of the angle between the hulls is 60°. Lastly, the largest angle, which is 90°, led to substantially lower performances. Figure 7 shows the overtopping analysis results through numerical simulation focused on wave overtopping discharge in the WaveCat reservoirs in the studies on wave overtopping involving the structures. The results obtained for the non-dimensional average overtopping discharge in the reservoir suggested that the described methodology could be used successfully to analyse the interaction between wave overtopping and WaveCat.

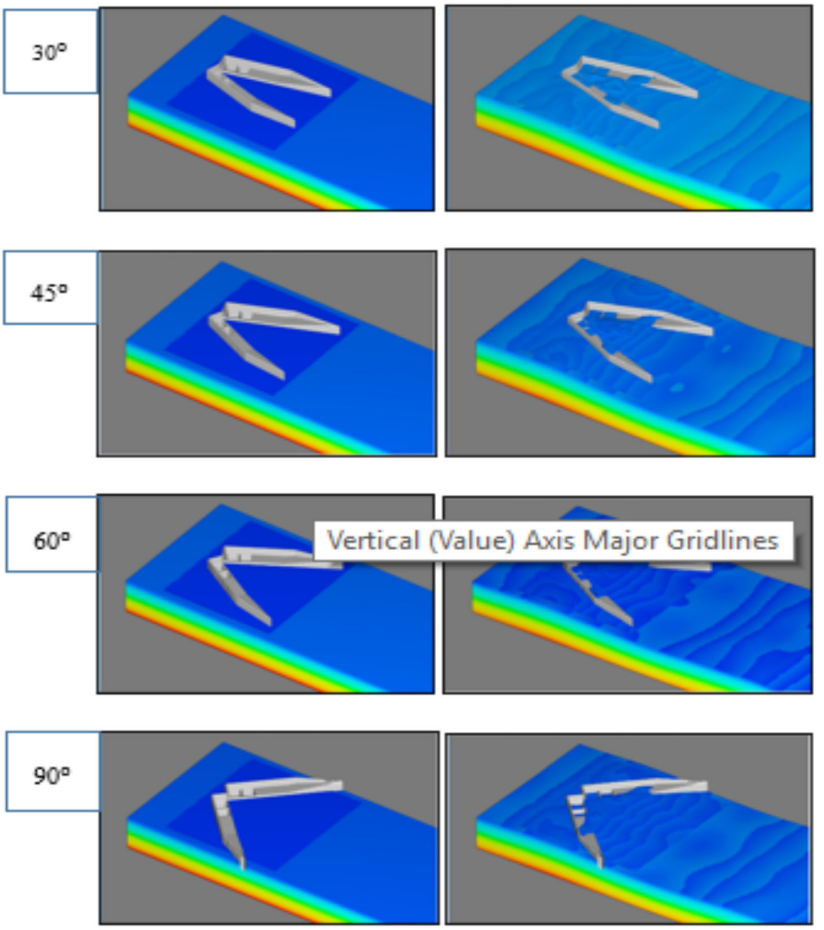

Figure 7: Overtopping behaviours of the reservoirs in numerical 3D for each wedge angle

Optimum Freeboard for Overtopping Discharge

In this case, the total overtopping discharge is simuated with the best wedge angle, which is 60°, obtained from Objective 2, and different freeboards. The overtopping discharge is strongly affected by the freeboard. Table 5 shows the freeboards used in the simulations.

Table 5: Freeboard input

Test ID	Freeboard, Rc (m)
1	0.02
2	0.04
3	0.07
4	0.09

Table 6 shows the non-dimensional overtopping discharge due to the non-dimensional freeboard.

Table 6: Overtopping discharge for each freeboard

Test ID	Wedge Angle (°)	Freeboard, *R**	Significant Wave Height, H_s *(m)*	Period, *(s)*	Overtopping Discharge	
					q (m^3/s)	*Q**
1	60	0.2	0.1	2.2	2.24	22.62
2	60	0.4	0.1	2.2	8.14×10^{-1}	8.22
3	60	0.7	0.1	2.2	1.36×10^{-1}	1.37
4	60	0.9	0.1	2.2	9.7×10^{-7}	9.79×10^{-6}

Figure 8 illustrates the non-dimensional wave overtopping rate in the reservoir of the simulated results. The distribution of the simulated data plotted in the graph is calculated using Equation 2. The results obtained for the non-dimensional average overtopping discharge in the reservoir, q reservoir, and freeboard, R_c, suggested that the described methodology could be used successfully to analyse the interaction between wave overtopping and WaveCat.

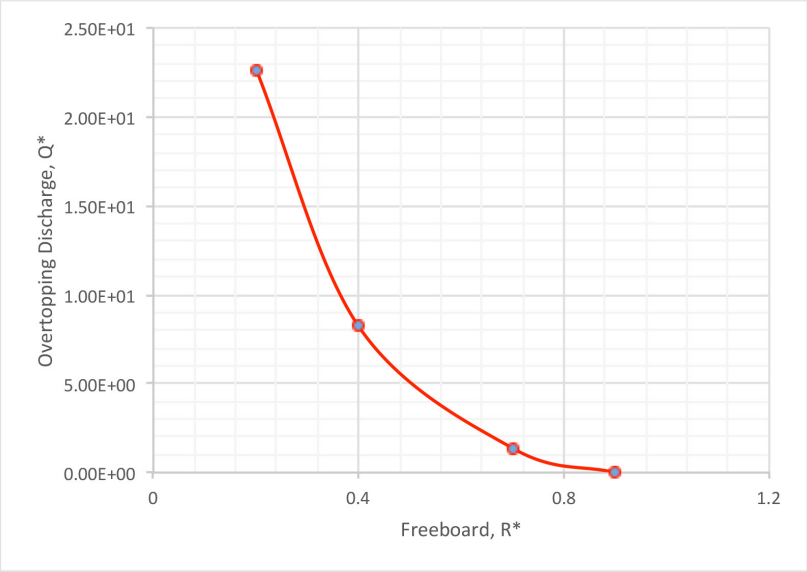

Figure 8: Non-dimensional overtopping discharge against dimensionless freeboard

The analysed result in this numerical simulation focuses on wave overtopping behaviour in both reservoirs by neglecting the studies on wave reflection and wave loading on the structures. Figure 8 also indicates that the simulated results show a good relationship between freeboard height, with height of 0.02 m and 0.09 m, and the overtopping discharge. Figure 8 shows that there is a negative correlation associated with the simulated results between non-dimensional average overtopping discharge in the reservoir, q reservoir, and freeboard, R_c. It is obvious as the crest freeboard height increases, the overtopping rate in the reservoir declines, and vice versa.

Conclusion

A numerical study of a WaveCat model to the scale of 1:30 was conducted using computational fluid dynamics. The main objective of this project is to investigate the overtopping performance of the WaveCat breakwater under different wedge angles and freeboards using computational fluid dynamics. The optimum wedge angle for overtopping discharge was obtained with the intermediate values of the angle between the hulls, 45° and 60°. In this simulation, the wave conditions used are Hs = 0.1 m and Tp = 2.2 s, and the optimum value of the angle between hulls obtained is 60°. Lastly, the largest angle, which is 90°, led to substantially lower performances. It can be concluded that the overtopping rate has high sensitivity to the angle between the hulls. The overtopping discharge is strongly affected by the freeboard, where the increment of the freeboard height will decrease the overtopping discharge rate. The overtopping phenomenon is affected by the height of crest freeboard and the significant wave height of the upcoming wave.

An initial stage of numerical simulation validation approach for the physical model test based on the previous study has reaffirmed the usability of the CFD Flow3D software as a modelling tool for analysing WaveCat. However, further study may be needed to clarify others geometrical and climate influences through both simulation and experimental approaches for the full deployment of the WaveCat wave energy converter.

References

Astariz, S., & Iglesias, G. (2015). Enhancing wave energy competitiveness through co-located wind and wave energy farms. A review on the shadow effect. In *Energies*. https://doi.org/10.3390/en8077344

Baquerizo, A., Losada, M. A., & Smith, J. M. (1998). Wave reflection from beaches: A predictive model. *Journal of Coastal Research*, *14*(1), 291–298.

Contestabile, P., Ferrante, V., & Vicinanza, D. (2015). Wave energy resource along the coast of Santa Catarina (Brazil). *Energies*, *8*(12), 14219–14243. https://doi.org/10.3390/en81212423

Cornett, A. (2009). A global wave energy resource assessment. *Sea Technology*.

Deilami-Tarifi, M., Behdarvandi-Askar, M., Chegini, V., & Haghighi-Pour, S. (2016). Modeling of the changes in flow velocity on seawalls under different conditions using FLOW-3D Software. *Open Journal of Marine Science*. https://doi.org/10.4236/ojms.2016.62026

Fernandez, H., Iglesias, G., Carballo, R., Castro, A., Fraguela, J. A., Taveira-Pinto, F., & Sanchez, M. (2012). The new wave energy converter WaveCat: Concept and laboratory tests. *Marine Structures*, *29*(1), 58–70. https://doi.org/10.1016/j.marstruc.2012.10.002

Folley, M., & Whittaker, T. J. T. (2009). Analysis of the nearshore wave energy resource. *Renewable Energy*. https://doi.org/10.1016/j.renene.2009.01.003

Haas, D. K. A., Fritz, D. H. M., French, D. S. P., Smith, D. B. T., & Neary, D. V. (2011). Assessment of Energy Production Potential from Tidal Streams in the United States Final Project Report Award Number : DE-FG36-08GO18174. *Georgia Tech Research Corporation*. https://doi.org/10.2172/1219367

Iglesias, G., & Carballo, R. (2010). Wave energy and nearshore hot spots: The case of the SE Bay of Biscay. *Renewable Energy*. https://doi.org/10.1016/j.renene.2010.03.016

Iglesias, Gregorio, Fernández, H., Carballo, R., & Castro, A. (n.d.). <*Wavecat Development. Pdf*>. *ii*, 2151–2158.

IRENA. (2014). Wave Energy Technology Brief. *IRENA Ocean Energy Technology Brief 4*, *June*, 28.

Jarocki. (2010). *Wave Energy Converter Performance Modeling and Cost of. March*.

Jarocki, D., & Wilson, J. H. (2010). Wave energy converter performance modeling and cost of electricity assessment. *ASME International Mechanical Engineering Congress and Exposition, Proceedings (IMECE)*. https://doi.org/10.1115/IMECE2010-37756.

Mathiesen, B. V., Lund, H., Connolly, D., Wenzel, H., Ostergaard, P. A., Möller, B., Nielsen, S., Ridjan, I., KarnOe, P., Sperling, K., & Hvelplund, F. K. (2015). Smart Energy Systems for coherent 100% renewable energy and transport solutions. In *Applied Energy*. https://doi.org/10.1016/j.apenergy.2015.01.075

Rusu, E., Pilar, P., & Guedes Soares, C. (2008). Evaluation of the wave conditions in Madeira Archipelago with spectral models. *Ocean Engineering*. https://doi.org/10.1016/j.oceaneng.2008.05.007

Shih, H. J., Chang, C. H., Chen, W. B., & Lin, L. Y. (2018). Identifying the optimal offshore areas for wave energy converter deployments in Taiwanese waters based on 12-year model hindcasts. *Energies*. https://doi.org/10.3390/en11030499

Sun, C., Shang, J., Luo, Z., Lu, Z., & Wang, R. (2018). A Review of Wave Energy Extraction Technology. *IOP Conference Series: Materials Science and Engineering*. https://doi.org/10.1088/1757-899X/394/4/042038

Tedd, J. (2007). Testing, analysis and control of Wave Dragon, Wave Energy Converter. *Civil Engineering*, *9*.

Tumin, A., Rusak, Z., & Fedorov, A. (2010). Theoretical fluid mechanics. In *AIAA Journal*. https://doi.org/10.2514/1.48391

Waters, R., Engström, J., Isberg, J., & Leijon, M. (2009). Wave climate off the Swedish west coast. *Renewable Energy*. https://doi.org/10.1016/j.renene.2008.11.016